

## Quadrupolar relaxation in $(\text{KBr})_{1-x}(\text{KCN})_x$

Z. Hu, D. Walton, and J. J. Vanderwal

*Department of Physics and the Institute for Materials Research, McMaster University,  
Hamilton, Ontario, Canada L8S 4M1*

(Received 16 December 1987; revised manuscript received 13 May 1988)

Brillouin scattering was used to study the dynamic properties of the mixed crystals  $(\text{KBr})_{1-x}(\text{KCN})_x$ . By analyzing the frequencies and linewidths of the  $T_{2g}$ -symmetry phonon, we were able to determine the cyanide quadrupolar relaxation rate as a function of temperature in the paraelastic regime. We found that this relaxation frequency is proportional to  $\exp(-1/T)$ , rather than proportional to the square root of temperature ( $\sqrt{T}$ ), as assumed in Michel's random-field theory. Modifying this theory by incorporating the observed temperature dependence of the relaxation rate improves the agreement with experimental data but is still not adequate. The hierarchically constrained relaxation model of Palmer *et al.*, on the other hand, does provide a phenomenological explanation for our data. In addition, we have determined the value of the random-field strength in these mixed systems.

### I. INTRODUCTION

In the mixed crystals  $(\text{KBr})_{1-x}(\text{KCN})_x$ , with cyanide concentration smaller than a critical value of  $x \sim 0.6$ , no structural phase transition occurs. Upon cooling from room temperature, the mixed crystals form an orientational glass state at a freezing temperature  $T_f$  which depends on cyanide concentration and probe frequency.<sup>1</sup> Volkmann *et al.*<sup>2</sup> have classified two distinguishable relaxation mechanisms in  $(\text{KBr})_{1-x}(\text{KCN})_x$  in terms of quadrupolar and dipolar processes. The freezing-in of dipoles and quadrupoles occurs at different temperatures.

The onset of the quadrupolar glass state is signaled by anomalies in the temperature dependence of the elastic susceptibilities. The most direct evidence is that the acoustic-phonon frequency, and corresponding elastic constant  $C_{44}$ , exhibit a minimum at  $T_f$ .<sup>3-7</sup> A plot of the probe frequency against the inverse of the quadrupolar freezing temperature for  $(\text{KBr})_{1-x}(\text{KCN})_x$  showed an Arrhenius behavior.<sup>2</sup> However, for  $x = 0.5$ , there are only three data points taken from Brillouin scattering,<sup>3</sup> neutron scattering,<sup>4</sup> and pendulum measurements;<sup>7</sup> thus, the value of the activation energy ( $\sim 8000$  K) for  $\text{CN}^-$  quadrupolar reorientation is uncertain.

A microscopic theory developed by Michel *et al.*<sup>8</sup> can explain anomalies in the elastic constant, but fails to yield maximum phonon attenuation at  $T_f$ , as revealed by Brillouin light scattering.<sup>9</sup> Recently Michel<sup>10</sup> has revised his theory by including the interaction between a random strain field and the orientational degrees of freedom of the cyanide ions in the microscopic Hamiltonian. He further demonstrated that the formation of the quadrupolar glass is due to the competing effect between the translation-rotation coupling and the random strain-rotation coupling. Very recent ultrasonic measurements<sup>11</sup> on elastic constants of three glassy mixed systems,  $\text{K}(\text{CN})_x\text{Br}_{1-x}$ ,  $\text{K}(\text{CN})_x\text{Cl}_{1-x}$ , and  $\text{Rb}(\text{CN})_x\text{Br}_{1-x}$ , have quantitatively verified this random-field model and

show that Michel's theory successfully accounts for, at least, the high-temperature static behavior of the elastic constants. Ultrasonic measurements as functions of temperature and frequency can also provide, in principle, valuable information on sound attenuation and relaxation processes. However, in  $(\text{KBr})_{1-x}(\text{KCN})_x$  with  $0.2 < x < 0.6$ , there is such heavy damping of the sound wave around  $T_f$  that the resulting signal loss prevents any attenuation measurements.

We have studied the dynamic properties of  $(\text{KBr})_{1-x}(\text{KCN})_x$  using Brillouin scattering. The strong damping of the sound wave around  $T_f$  is revealed in the temperature-dependent broadening of the phonon linewidth. Combining both phonon-frequency and attenuation data, we are able to determine the  $\text{CN}^-$  quadrupolar relaxation rate as a function of temperature. The phonon attenuation has been analyzed using Michel's random-field theory, and Palmer *et al.*'s theory of hierarchically constrained relaxation. We will show that the  $\text{CN}^-$  quadrupolar relaxation rate in mixed crystals is proportional to  $\exp(-1/T)$ , rather than  $\sqrt{T}$ , as assumed by Michel.<sup>10</sup> With this modification to Michel's model, the calculated phonon linewidths are in improved agreement with the experimental data. However, it is impossible to account for the results with a single relaxation time, and we will show that a hierarchical relaxation process where the relaxation of a CN ion is constrained by that of other ions provides a promising model at low temperatures.

### II. EXPERIMENTAL

The single crystals were grown at the Crystal Growth Laboratory of the University of Utah. Samples were cleaved along the  $\{100\}$  planes and typically had dimensions of  $4 \times 4 \times 4$  mm<sup>3</sup>. The samples were put under vacuum as quickly as possible so that the surface of the crys-

tal would not deteriorate by exposure to moisture in the air.

The Brillouin-scattering technique employed has been described in detail elsewhere.<sup>9</sup> A stabilized single-frequency argon-ion laser provided the exciting radiation at 5145 Å. The scattered light was analyzed with a piezoelectrically scanned four-pass tandem Fabry-Perot interferometer. The dynamic scanning and mirror alignment of this interferometer were controlled by a micro-computer. The signal was detected by a cooled photomultiplier tube and the data stored in the computer via an analog-to-digital converter. In order to measure the spectra of the  $T_{2g}$  phonons, which propagate along the [110] direction and are polarized in the [001] direction, a 90° scattering geometry was employed. The (100) and (010) surfaces of the sample were perpendicular to the incident and the scattered light, respectively.

The sample was cooled using a continuous-flow He cryostat which was mounted directly above a standard liquid-helium storage vessel. The temperature of the sample could be varied from 4.2 to 300 K by adjusting the rate of helium-gas flow. Additional fine temperature control was achieved using a resistance heater and a temperature controller. Temperatures were measured using both a thermocouple and silicon diode. The error in temperature measurements is about 1 K.

The linewidths were determined by fitting the Brillouin peak using the convolution of a Lorentzian-shaped phonon profile with an instrumental function. Considering the variation of the instrumental finesse and fitting errors, the phonon-linewidth measurements were accurate to within 15 MHz.

The acoustic-phonon frequency ( $\nu$ ) can be converted to the velocity of sound ( $v$ ) by the Brillouin-scattering equation,<sup>12</sup>

$$\nu = \frac{2nv \sin(\theta/2)}{\lambda_0}, \quad (1)$$

where  $\lambda_0$  is the incident laser wavelength,  $n$  is the index of refraction, and  $\theta$  is the scattering angle. The elastic constant ( $C_{44}$ ) is related to the velocity of sound ( $v$ ) by<sup>12</sup>

$$C_{44} = \rho v^2, \quad (2)$$

where  $\rho$  is the density of the sample. Thus  $\nu$ ,  $v$ , and  $C_{44}$  are interchangeable via Eqs. (1) and (2).

### III. RESULTS AND DISCUSSION

#### A. Quadrupolar relaxation rate

The frequency (stars) and the full width at half maximum (FWHM) (open circles) of the transverse-acoustic phonon with  $T_{2g}$  symmetry, for the  $x=0.35$  sample, are shown in Fig. 1 as functions of temperature. The data for  $x=0.5$ , from Ref. 9, are also presented in Fig. 2 for comparison. The general features in these figures are the occurrence of a minimum in phonon frequency and a maximum in phonon width at around  $T_f$ . Here we focus our attention on the temperature range above  $T_f$  and will refer to this range as the paraelastic regime.

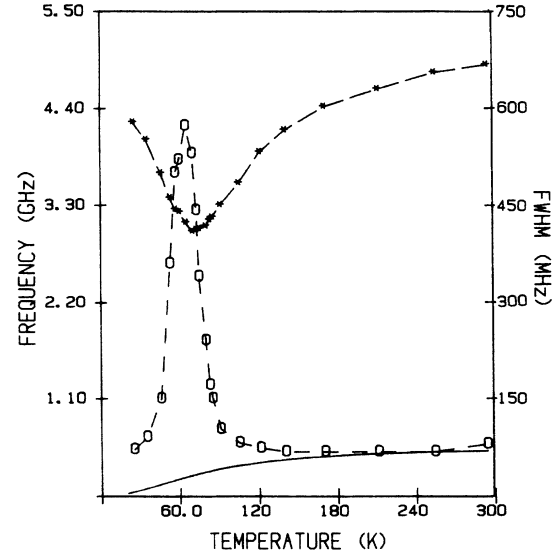


FIG. 1. Brillouin shift (\*) and full width at half maximum (FWHM) (○) of the acoustic phonon with  $T_{2g}$  symmetry for  $x=0.35$  are plotted against temperature. The dashed lines are guides to the eye. The solid line is the phonon linewidth due to pure lattice-anharmonic effect.

Following Michel's theory,<sup>10</sup> the  $\text{CN}^-$  orientational modes are strongly coupled to the  $T_{2g}$  phonon modes. The bilinear translational-rotational coupling results in the softening of the elastic constant. In the paraelastic region, this effect on the elastic constant may be generally expressed as<sup>13,14</sup>

$$C_{44} = C_{44}^0 - \frac{\Delta C_{44}}{1 + i\omega\tau}, \quad (3)$$

where  $C_{44}^0$  is the bare elastic constant,  $\Delta C_{44}$  represents

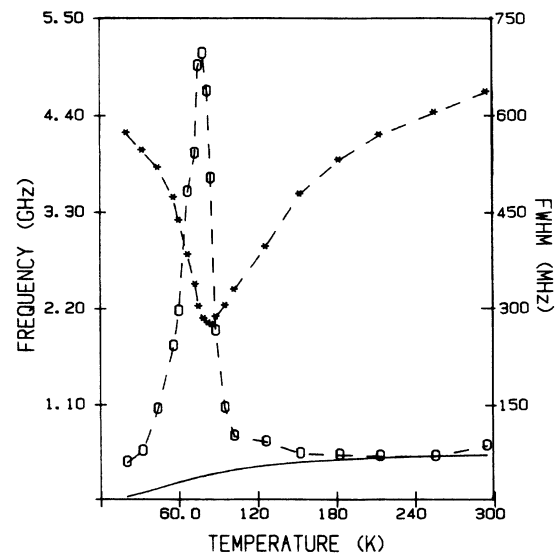


FIG. 2. The temperature dependence of the Brillouin shift (\*) and width (○) of the  $T_{2g}$  phonon for  $x=0.5$ , from Ref. 9. The dashed lines are guides to the eye, and the solid line is identical to the one in Fig. 1.

the temperature dependence of the coupling,  $\omega$  is the angular phonon frequency ( $2\pi\nu$ ), and  $\tau$  is the relaxation time of the excitations which are coupled to the phonons. In this case, the excitations are  $\text{CN}^-$  orientational modes.

Equation (3) can be further separated into a real part,

$$\text{Re}C_{44} = C_{44}^0 - \frac{\Delta C_{44}}{1 + \omega^2\tau^2}, \quad (4)$$

and an imaginary part,

$$\Gamma(T) - \Gamma_0 = \frac{q}{2\pi\rho} \text{Im}C_{44} = \frac{\tau\Delta C_{44}}{1 + \omega^2\tau^2} \frac{q^2}{2\pi\rho}, \quad (5)$$

where  $q$  is the phonon wave vector,  $\Gamma$  is the phonon width, and  $\Gamma_0$  represents additional sound attenuation not due to the quadrupolar-phonon interaction. Combining Eqs. (4) and (5), the relaxation rate can be expressed as<sup>13,14</sup>

$$\frac{1}{\tau} = \left| \frac{C_{44}^0 - C_{44}(T)}{\Gamma - \Gamma_0} \right| \frac{q^2}{2\pi\rho}. \quad (6)$$

When one considers anharmonic effects, the  $C_{44}^0$  in Eq. (6) is replaced with a temperature-dependent bare elastic constant of the  $\text{CN}^-$ -free reference system  $\text{KBr}$ , given by<sup>6</sup>

$$C_{44}^0(T) = C_{44}^0 \left[ 1 + \alpha_{44} \frac{\Theta_D}{e^{\Theta_D/T} - 1} \right], \quad (7)$$

where  $\alpha_{44} = -1.8 \times 10^{-4} \text{ K}^{-1}$ ,  $C_{44}^0 = 5.11 \times 10^9 \text{ N/m}^2$ , and  $\Theta_D = 125 \text{ K}$ , after Ref. 6.

The anharmonic effect on the phonon linewidth  $\Gamma_0$  may be estimated by use of the relaxation expression<sup>15</sup>

$$\Gamma_0(T) = \frac{\gamma^2 \omega^2 T K}{\pi \rho v^4} \frac{1}{1 + \omega^2 \tau_T^2}, \quad (8)$$

where  $K$  is the thermal conductivity,  $\tau_T$  is the thermal phonon lifetime,  $v$  is the velocity of the sound, and  $\gamma$  is the Grüneisen constant. Using the experimental values of the specific heat and thermal conductivity of  $\text{KBr}$ ,<sup>16</sup> one finds  $\omega\tau_T \sim 1$  around 80 K. The calculation of Eq. (8) yields the solid lines shown in Figs. 1 and 2; these have typical shapes for anharmonic linewidths observed in light-scattering measurements.<sup>15,17</sup>

Using Eqs. (2) and (6), and  $2\pi\nu = \nu q$ , we further obtain

$$\frac{1}{\tau} = \frac{2\pi[\nu_0^2(T) - \nu^2(T)]}{\Gamma(T) - \Gamma_0(T)}, \quad (9)$$

where  $\nu(T)$  and  $\Gamma(T)$  are the measured phonon frequency and linewidth, respectively.  $\nu_0$  is the bare phonon frequency converted from the elastic constant in Eq. (7) via Eqs. (1) and (2).  $\Gamma_0$  is given by Eq. (8).

The quadrupolar relaxation rate was thus calculated, using Eq. (9), as a function of temperature. The results are shown in Fig. 3: stars and open circles are for the  $x = 0.5$  and 0.35 samples, respectively. Solid and dashed lines are best fits to the data with an Arrhenius relaxation:  $1/\tau = (1/\tau_0) \exp(-E_0/k_B T)$ . Two regimes may be distinguished above  $T_f$ , and at the highest temperatures

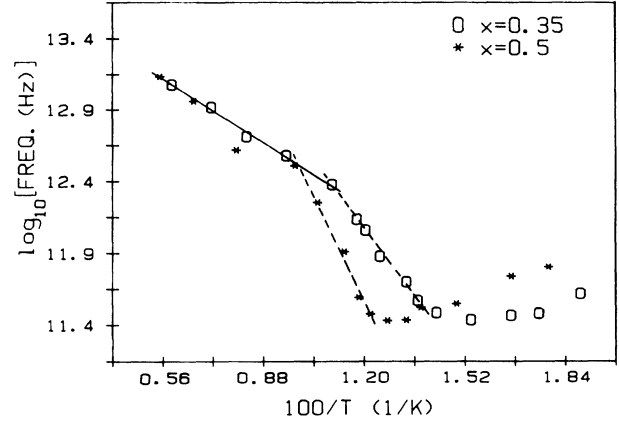


FIG. 3. The logarithm of the quadrupolar-relaxation frequency, against  $1/T$ . Stars are for the  $x = 0.5$  sample and open circles for the  $x = 0.35$  sample. Solid and dashed lines are best fits to the data with an Arrhenius relation in two temperature regimes.

both concentrations have the same temperature dependence. A straight line through the points yields an activation energy of 318 K and a preexponential of  $2.2 \times 10^{13} \text{ Hz}$ . Below about 100 K for  $x = 0.5$  and 90 K for  $x = 0.35$ , another straight-line region appears which leads to two different activated processes with activation energies of 981 K for  $x = 0.5$  and 608 K for  $x = 0.35$ . The preexponentials, however, are  $5 \times 10^{16}$  and  $2 \times 10^{15} \text{ Hz}$ , respectively, indicating that we are no longer dealing with a single-particle process. Below  $T_f$  the single Debye relaxation approximation has clearly broken down. When the temperature is lower than  $T_f$  for  $(\text{KBr})_{1-x}(\text{KCN})_x$ , the random strain field will become dominant and suppress translation-rotation bilinear coupling.<sup>10</sup> Thus Eq. (3) is no longer valid at  $T < T_f$ .

Our values are considerably smaller than the previously reported ones,<sup>2</sup> namely,  $E_0 \sim 8000 \text{ K}$  and  $1/\tau_0 \sim 10^{60} \text{ Hz}$  for the  $x = 0.5$  sample. Those values were obtained by comparing three data points from neutron scattering,<sup>4</sup> Brillouin scattering,<sup>3</sup> and torsion pendulum<sup>7</sup> measurements. We argue that this comparison may not be valid. The reason is due to a dramatic change in probe frequency: the propagation of sound is an adiabatic process for the frequencies greater than the Megahertz range, while the pendulum resonance probes an isothermal relaxation process, due to its very low frequency (100 Hz). It is not valid to directly compare the adiabatic and isothermal relaxation times.<sup>18</sup>

## B. Acoustic-phonon linewidth

On the basis of a microscopic model, the dynamic properties of  $(\text{KBr})_{1-x}(\text{KCN})_x$  were investigated by Michel.<sup>10</sup> The phonon width ( $\Gamma$ ) which is associated with the attenuation of the sound wave is given by<sup>10</sup>

$$\Gamma = \omega \Delta_{11} f(\omega) \quad (10)$$

with

$$f(\omega) = \frac{\lambda}{\omega^2 + \lambda^2} \quad (11)$$

and

$$\Delta_{11} = M_{11} \left[ 1 - \frac{D_{11}}{M_{11}} \right], \quad (12)$$

where  $M_{11}$  is the bare phonon frequency,  $\lambda$  is the cyanide quadrupolar relaxation rate,  $\omega$  is the probe frequency, and  $\Delta_{11}$  describes an effective interaction among  $\text{CN}^-$  quadrupoles.  $D_{11}$  is the renormalized phonon frequency and can be further expressed as

$$D_{11} = \frac{(1 - \chi^0 \delta) M_{11}}{1 + (J + C^S) \chi^0} \quad (13)$$

with

$$\chi^0 = \frac{x Y_w}{T} \left[ 1 - \frac{x(1-x)}{T^2} \xi_w h^2 \right], \quad (14)$$

where  $\chi^0$  denotes the single-particle orientational susceptibility.  $Y_w$  and  $\xi_w$  are single correlation functions,  $x$  is the cyanide concentration, and  $\delta$  is the effective translation-rotation coupling.  $J$  and  $C^S$  describe the orientational self-energy correction, and  $h$  is the strength of the random strain field induced by the difference in ionic radii between  $\text{CN}^-$  and  $\text{Br}^-$  ions.

The experimental phonon widths, from which were subtracted the anharmonic part  $\Gamma_0$ , are shown in Figs. 4 and 5 for  $x=0.35$  and  $0.5$ , respectively. The theoretical curves calculated using Eqs. (10)–(14) are shown for comparison in Figs. 4 and 5 as dashed lines. The parameters used are directly taken from Refs. 10 and 19:  $\delta=2357$  K,  $\xi_w \sim 0.06$ ,  $Y_w \sim 0.08$ ,  $C^S=928$  K, and  $J=828$  K. The quadrupolar relaxation rate is given by Michel:<sup>10</sup>

$$\lambda = 6.45 \times 10^{10} \sqrt{T}. \quad (15)$$

The strength of the random field ( $h$ ) was within a range  $300 \text{ K} \leq h \leq 400 \text{ K}$ , as calculated from the microscopic potential by Michel. We found that  $h=400$  K, the upper limit of the theoretical value, better describes the data.

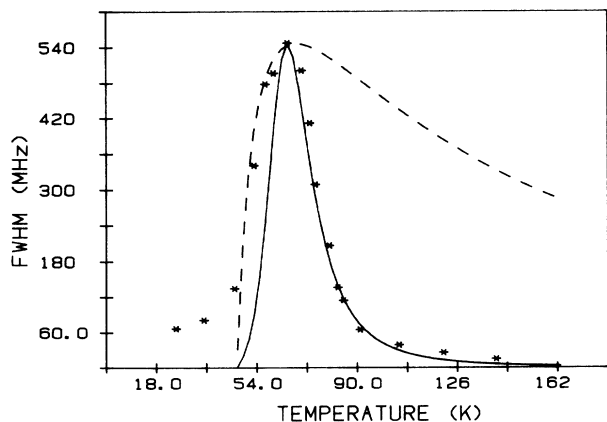


FIG. 4. The phonon linewidths are plotted against temperature for  $x=0.35$ . Stars are experimental data which were corrected for an anharmonic damping contribution. The dashed line is the calculated curve from Michel's theory. The solid line is the present calculation.

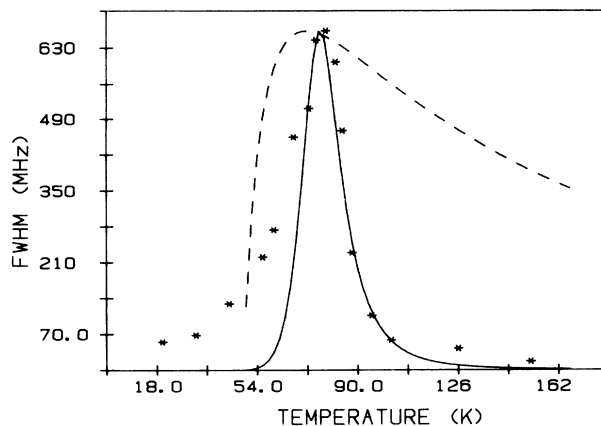


FIG. 5. The phonon linewidths are plotted against temperature for the  $x=0.5$  sample. The symbols are the same ones used in Fig. 4.

As evidenced in Figs. 4 and 5, the theoretical curves exhibit a similar maximum to those of the experimental data. However, there are large differences in their overall features. In particular, the theoretical linewidths are much higher than the experimental ones at  $T$  above  $T_f$ .

Motivated by the analysis presented in the last section, we changed the theoretical relaxation rate  $\lambda$  in Eq. (15) into the Arrhenius expression

$$\lambda = \lambda_0 \exp(-E_0/k_B T). \quad (16)$$

Substituting Eq. (16) into Eq. (11) and keeping other theoretical values as they are, we recalculated the phonon linewidth with  $\lambda_0$  and  $E_0$  as fitting parameters. The results are shown in Figs. 4 and 5 for  $x=0.35$  and  $0.5$  as solid lines.  $E_0$  and  $\lambda_0$  turn out to be  $960$  K and  $3.4 \times 10^{14}$  Hz, respectively, for  $x=0.5$  and  $610$  K and  $2.3 \times 10^{14}$  Hz for  $x=0.35$ . It is clear from these figures that the modified theoretical curves fit the experimental data much better. It is interesting that the activation energies correspond closely to those obtained from the second region referred to above.

There are still some discrepancies, however, between the modified theoretical lines and the data, especially in the low-temperature region. These may be due to several reasons. Firstly, Michel's theory is based on classical statistical mechanics and is not applicable at low temperatures where a quantum-mechanical treatment is required,<sup>10</sup> although this would not be expected to become a problem until temperatures are reached which are much lower than those involved here. Secondly, the single relaxation approximation employed here may not work at  $T$  close to  $T_f$ . There is evidence for a breakdown of a single-particle relaxation process in the very high preexponentials obtained from Arrhenius plots in this region.

A broad distribution of relaxation times and barrier heights could be used. This kind of broad relaxation spectrum has, in fact, been observed in the dielectric properties of  $(\text{KBr})_{1-x}(\text{KCN})_x$  (Ref. 20) and in other glassy crystals.<sup>17</sup>

### C. Hierarchically constrained model

Data of this sort can always be modeled by a distribution of relaxation times, but as Palmer *et al.*<sup>21</sup> pointed out, these distributions are appropriate for parallel processes, whereas in glasses and many other systems it is expected that relaxation is a serial process with relaxation of one level being constrained by relaxation of other levels. Palmer *et al.* discussed various possible models, and developed expressions for a process of relaxation of a multilevel system of  $N$  Ising spins (or pseudospins) such that the number of spins in level  $n$  is  $N_n$ , and  $N_{n+1} = N_n/\lambda$  where  $\lambda$  is a constraint greater than 1.

Each spin in level  $n+1$  is only free to change its state if  $\mu_n$  spins in level  $n$  attain one particular state of their  $2^n$  possible ones. The relaxation times in the theory of Palmer *et al.* are related by

$$\tau_{n+1} = 2^{\mu_n} \tau_n \quad (17)$$

leading to

$$\tau_n = \tau_0 2^{\sum_{k=\mu_k}^{n-1} (\dots)} \quad (18)$$

The relaxation function

$$N^{-1} \sum_{i=1}^N \langle S_i(0) S_i(t) \rangle \quad (19)$$

is

$$q(t) = \sum_{n=0}^{\infty} (N_n/N) \exp(-t/\tau_n). \quad (20)$$

We wish to report the results of using the theory of Palmer *et al.* to account for our data. Specifically we wish to account for the phonon widths using hierarchically constrained relaxation processes for which  $\tau_0$  is given by a single relaxation time expression provided by the high-temperature portion of the data in Fig. 3. This is obtained from the solid line shown, and is

$$\tau_0 = 8.5 \times 10^{-13} e^{318/T}. \quad (21)$$

Our results are in the frequency domain so we require the transform of Eq. (20):

$$Q(\omega) = \sum_{n=0}^{\infty} N_n/N (1 - i\omega\tau_n)^{-1}. \quad (22)$$

In order to obtain a finite limit to  $\tau$ ,  $\mu_n$  must decrease as  $n$  increases. Palmer *et al.*<sup>21</sup> suggest that

$$\mu_n = \mu_0/(n+1)^p \quad (23)$$

and

$$\tau_n = \tau_0 (2^{\mu_0} 2^{\mu_1} \dots 2^{\mu_{n-1}}) = \tau_0 (2^{\sum_{k=1}^{n-1} (\mu_0/k^p)}), \quad (24)$$

where  $(p-1) \ll 1$ . In order to proceed further it is necessary to evaluate

$$\sum_{k=0}^{n-1} (k+1)^{-p}. \quad (25)$$

If  $p=1$ , a more or less useful expression results, whose

usefulness increases as  $n$  increases. Palmer *et al.*, arguing that  $n$  is large, obtain an expression for  $q(t)$  by replacing the sum over  $n$  in Eq. (22) by an integral. Zwanzig<sup>22</sup> has questioned the accuracy of this approximation; however, Palmer *et al.*, in their reply,<sup>23</sup> argue that the integral has greater physical significance, and that the sum is only a device to introduce the model.

Following this philosophy, we assume that the levels are closely spaced and numerous. Although it is not difficult to evaluate the sum of Eq. (22), we also prefer it to be an integral. Palmer *et al.* propose that  $p$  should increase with temperature. In order to evaluate Eq. (24) for any value of  $p$  we must replace that sum by an integral as well:

$$s = \sum_{k=0}^{n-1} 1/(k+1)^p = \int_1^n dk/k^p = (n^{1-p} - 1)/(1-p) \quad (26)$$

if  $p = 1 + \epsilon$ , where  $\epsilon$  is  $\ll 1$ , and

$$s = \{1 - [1 - (1 - 1/n)]^\epsilon\} / \epsilon, \quad (27)$$

$$s \cong \ln(n) + \epsilon(1 - 1/n)^2/2.$$

Assuming  $\epsilon$  to be small we neglect the second term, and Eq. (22) becomes

$$Q(\omega) = \int_0^\infty dn / (1 - i\omega\tau_0 n^{\mu_0}) \lambda^n. \quad (28)$$

Therefore, Eq. (3) can be rewritten as

$$C_{44} = C_{44}^0 - \Delta C_{44} Q(\omega). \quad (29)$$

The next step is to use this equation to deduce the phonon width, using the change in phonon frequency to eliminate the coupling constant  $\Delta C_{44}$ . The value of  $\tau_0$  is provided by the fit to the high-temperature portion of the data where a single relaxation time provides a good approximation. Thus two adjustable constants remain,  $\lambda$  and  $\mu_0$ . A microscopic model should provide a value for  $\lambda$ . We do not wish to discuss this question in detail, but it is worth remarking that if the levels  $n$  are associated with fluctuations in the concentration,  $\lambda$  should be on the order of  $1/x$ .

We are particularly interested in the temperature dependence of  $\mu_0$  since this measures the degree to which the spins are constrained. We expect  $\mu_0$  to increase from zero at high temperatures to high values at temperatures below the glass transition temperature where the interaction between the spins becomes important. For  $\lambda$  less than one it was impossible to fit the data. If it were greater than 2.5, abrupt discontinuities in the value of  $\mu_0$  appeared at low temperatures. If a smooth monotonic increase in  $\mu_0$  was desired, the value of  $\lambda$  had to be 1.9 for  $x=0.5$  and 2.2 for  $x=0.35$ .

The results are displayed in Fig. 6. As expected,  $\mu_0$  increases from zero as the temperature is lowered. What is interesting is that this increase begins abruptly at a temperature higher than  $T_f$  at the temperature where the onset of CN interaction occurs, as discussed above.

$T_f$  is dependent on the probe frequency,<sup>1</sup> increasing with frequency. For the frequencies of the phonons in-

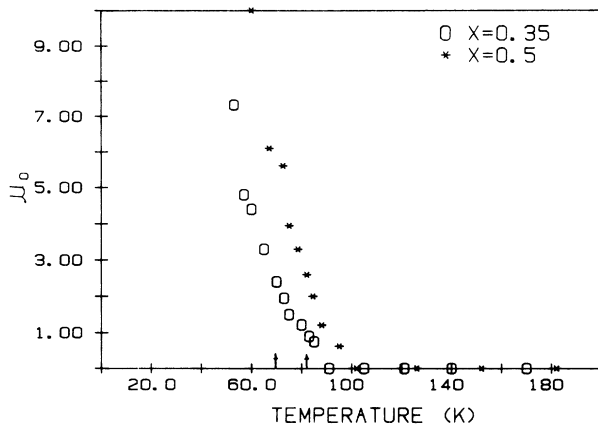


FIG. 6. The value of  $\mu_0$  necessary to obtain the correct phonon attenuation from a single relaxation process whose temperature dependence is given by the solid line in Fig. 3, plotted against temperature. The temperatures of the glass transition are indicated by the two arrows.

involved in Brillouin scattering,  $T_f$ , deduced from the temperature of the minimum in phonon frequency, is 83 K for  $x=0.5$  and 70 K for  $x=0.35$ .

A value for  $\mu_0$  close to zero indicates that the constraint imposed on a spin by its companions is negligible, and that a single relaxation time governs the spin dynamics. The departure from zero signals the onset of important interactions. The fact that this occurs not at  $T_f$  for our data but at a higher temperature  $T_{\text{int}}$  indicated that interaction between the CN ions begins above  $T_f$ . This can be understood if  $T_{\text{int}}$  corresponds to the temperature at which the relaxation of a single spin is first affected by that of its neighbors.  $T_f$ , on the other hand, is determined by the temperature at which the relaxation rate becomes comparable to the phonon frequency. Thus  $T_f$  should be frequency dependent but  $T_{\text{int}}$  should not. It would be useful to test this result with ultrasonic data. Unfortunately, while ultrasonic data are available for the frequency shift, none are available for the attenuation at these concentrations.

#### IV. SUMMARY AND CONCLUSION

The Brillouin-scattering technique was used to study the dynamic elastic properties of the mixed crystals  $(\text{KBr})_{1-x}(\text{KCN})_x$  for  $x=0.35$  and  $0.5$ . Near the quadrupolar glass freezing temperature, the phonon frequency and attenuation of the sound waves corresponding to the  $C_{44}$  elastic constant exhibit a minimum and a maximum, respectively. Combining the phonon frequency with the damping data, we extracted the cyanide quadrupolar relaxation rate as a function of temperature in the paraelastic regime, and found that this rate follows an Arrhenius relation.

We have calculated the phonon linewidth based on Michel's microscopic theory. The results show a maximum at  $\sim T_f$ , similar to our experimental results. However, at  $T > T_f$ , the theoretical widths are much larger than the experimental values. We changed the relation of the quadrupolar relaxation rate ( $1/\tau$ ) versus temperature ( $T$ ) from  $1/\tau \propto \sqrt{T}$ , as assumed by Michel's theory, to  $1/\tau \propto \exp(-1/T)$ , as obtained by analysis of our Brillouin data. With this modification to Michel's theory, the calculated widths are in better agreement with the data. However, complete agreement was achieved using the model of Palmer *et al.* of hierarchically constrained relaxation. At the present stage this model is clearly phenomenological. It would appear that a satisfactory microscopic description may be achieved by incorporating the model of Palmer *et al.* into the Michel theory. However this is beyond the scope of the present work.

We also determined that the strength of the random field in  $(\text{KBr})_{1-x}(\text{KCN})_x$  is about 400 K, the upper limit estimated from the microscopic potential in Ref. 10. We thus provide new experimental evidence to support the random-field model; the formation of the orientational glass state depends on a delicate balance between the translation-rotation coupling and the random-field  $\text{CN}^-$ -pseudospin coupling. When  $T < T_f$ , the latter becomes dominant, the ferroelastic order transition is suppressed, and the  $\text{CN}^-$  are frozen in by high hindering barriers.

#### ACKNOWLEDGMENTS

We wish to thank Dr. K. Knorr, Dr. C. W. Garland, and Dr. J. O. Fossum for helpful discussions. This work was supported by a grant from the Natural Science and Engineering Research Council of Canada.

<sup>1</sup>A. Loidl, R. Feile, and K. Knorr, Phys. Rev. Lett. **48**, 1263 (1982).

<sup>2</sup>U. G. Volkman, R. Böhmer, A. Loidl, K. Knorr, U. T. Höchli, and S. Haussühl, Phys. Rev. Lett. **56**, 1716 (1986).

<sup>3</sup>S. K. Satija and C. H. Wang, Solid State Commun. **28**, 617 (1978).

<sup>4</sup>J. M. Rowe, J. J. Rush, D. G. Hinks, and S. Susman, Phys. Rev. Lett. **43**, 1158 (1979).

<sup>5</sup>C. W. Garland, J. Z. Kwicien, and J. C. Damien, Phys. Rev. B **25**, 5818 (1982).

<sup>6</sup>R. Feile, A. Loidl, and K. Knorr, Phys. Rev. B **26**, 6875 (1982).

<sup>7</sup>K. Knorr, U. G. Volkman, and A. Loidl, Phys. Rev. Lett. **57**, 2544 (1986).

<sup>8</sup>K. H. Michel, J. Naudts, and B. DeRaedt, Phys. Rev. B **18**, 648 (1978).

<sup>9</sup>J. J. Vanderwal, Z. Hu, and D. Walton, Phys. Rev. B **33**, 5782 (1986).

<sup>10</sup>K. H. Michel, Phys. Rev. Lett. **57**, 2188 (1986); Phys. Rev. B **35**, 1405 (1987); **35**, 1414 (1987).

<sup>11</sup>J. O. Fossum and C. W. Garland, Phys. Rev. Lett. **60**, 592

- (1988).
- <sup>12</sup>W. Hayes and R. Loudon, *Scattering of Light by Crystals* (Wiley, New York, 1978).
- <sup>13</sup>P. W. Young and J. F. Scott, *Phase Transitions* **6**, 175 (1986).
- <sup>14</sup>M. S. Zhang, T. Yagi, W. F. Oliver, and J. F. Scott, *Phys. Rev. B* **33**, 1381 (1986).
- <sup>15</sup>J. P. Bonnet, M. Boissier, C. Vedel, and R. Vacher, *J. Phys. Chem. Solids* **44**, 515 (1983).
- <sup>16</sup>*Thermophysical Properties of Matter*, edited by Y. S. Touloukian *et al.* (Plenum, New York, 1970), Vols. 2 and 5.
- <sup>17</sup>E. Courtens, F. Huard, and R. Vacher, *Phys. Rev. Lett.* **55**, 722 (1985).
- <sup>18</sup>Y. H. Jeong, S. R. Nagel, and S. Bhattacharya, *Phys. Rev. A* **34**, 602 (1986).
- <sup>19</sup>K. H. Michel, *Z. Phys. B* **61**, 45 (1985).
- <sup>20</sup>N. O. Birge, Y. H. Jeong, S. R. Nagel, S. Bhattacharya, and S. Susman, *Phys. Rev. B* **30**, 2306 (1984).
- <sup>21</sup>P. G. Palmer, D. L. Stein, E. Abrahams, and P. W. Anderson, *Phys. Rev. Lett.* **53**, 958 (1984).
- <sup>22</sup>R. Zwanzig, *Phys. Rev. Lett.* **54**, 364 (1985).
- <sup>23</sup>P. G. Palmer, D. L. Stein, E. Abrahams, and P. W. Anderson, *Phys. Rev. Lett.* **54**, 365 (1985).